AD-A136 027 EFFECT OF THE OVERLOAD RATIO ON FATIGUE GROWTH BEHAVIOR 1/1
IN TI-6A1-4V(U) FOREIGN TECHNOLOGY DIV WRIGHT-PATTERSON
AFB OH O JIE ET AL. 17 NOV 83 FTD-ID(RS)T-1578-83

UNCLASSIFIED F/G 11/6 NL

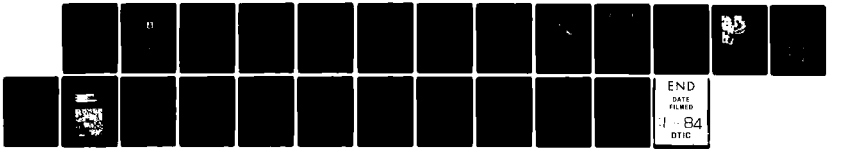

END
DATE FILMED
1-84
DTIC

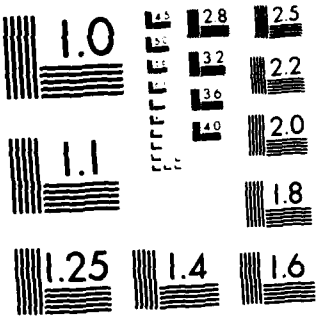

FTD-ID(RS)T-1578-83

FOREIGN TECHNOLOGY DIVISION

EFFECT OF THE OVERLOAD RATIO ON FATIGUE GROWTH BEHAVIOR IN Ti-6Al-4V

by

O. Jie, S. Deyu and Y. Minggao

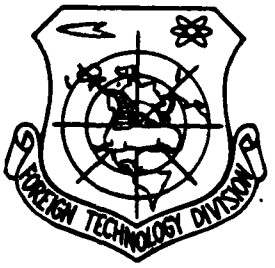

EDITED TRANSLATION

FTD-ID(RS)T-1578-83 17 November 1983

MICROFICHE NR: FTD-83-C-001399

EFFECT OF THE OVERLOAD RATIO ON FATIGUE GROWTH BEHAVIOR IN Ti-6Al-4V

By: O. Jie, S. Deyu and Y. Minggao

English pages: 20

Source: Hangkong Cailiao Yanjiusuo, Vol. 2, Nr. 1, June 1982, pp. 31-39; 12-14

Country of origin: China
Translated by: LEO KANNER ASSOCIATES
F33657-81-D-0264
Requester: FTD/TQTA

PREPARED BY:

TRANSLATION DIVISION
FOREIGN TECHNOLOGY DIVISION
WP-AFB, OHIO.

GRAPHICS DISCLAIMER

All figures, graphics, tables, equations, etc. merged into this translation were extracted from the best quality copy available.

Effect of the Overload Ratio on Fatigue Growth Behavior in Ti-6Al-4V

Ouyang Jie, Song Deyu and Yan Minggao

Abstract

This paper studies the effects of different tensile overload ratios, $r=P_{oL}/P_{cA}$, on the fatigue crack growth process and rate of sheet titanium alloy TC_4. It also investigates the law of the overload retardation effect which changes with the changes of the overload ratio. After further analyzing the main factors influencing the overload retardation effect, we proposed a diagram of the process and mechanism of overload retardation fatigue crack growth. Moreover, we obtained an empirical relational formula to calculate the maximum plastic strain (ε_{3max}) of the overload crack tip as well as the crack growth life (N_D) lengthened because of the overloading.

I. Preface

Tests and use of aeronautical materials and parts show that the changes of loading amplitude and variable load sequence produce complex effects on the process of fatigue crack growth and that tensile overload can retard the growth rate of fatigue cracks [1-4]. There are many factors which influence overload retardation effects and among them the deciding factor is the overload ratio, $r=P_{oL}/P_{cA}$ [4-5]. A great deal of work has shown that during the fatigue crack growth process, the single or multiple exertions of tensile overload begin to produce retardation effects when the overload ratio reaches a certain threshold value (generally about 1.5); when it increases to 2.0, the retardation effect noticeably rises; when further increased to about 2.5, this can cause the crack growth rate to rise several to several ten fold; when the overload ratio approaches or reaches 3.0, this can cause the crack to basically stop or

completely stop growth and thus greatly lengthen the crack growth life. It can be seen that the life predictions of parts operating under variable load, if we do not take into consideration the overload retardation effect, can obtain conservative results.

Different mechanisms [4, 6-11] have been proposed for the causes of overloading producing retardation effects including crack tip passivation, residual compression stress, crack tip closure effects and strain strengthening etc. To date, all of the mathematical models for estimating the overload effects have been separately proposed [9, 12-15] using one certain mechanism as the basis. Recently, we proposed a multifactor complex mechanism caused by the overload plastic strain which takes the residual pressure stress in front of the crack tip and the closure stress in back of the crack tip as predominant [2].

The aim of this work is to further reveal the process and mechanism of the overload's retardation crack growth rate after studying the effects of the overload ratio on the fatigue crack growth of TC_4 titanium alloy. This more realistically estimates the overload retardation effects and provides beneficial materials.

II. Test Process

The tests used TC_4 (Ti-6Al-4V) sheet titanium alloy, an annealing state and the thickness was 2mm. Its main chemical composition was: 5.94%Al, 4.25%V, 0.11%Fe, $<$0.05%Si, and the rest was Ti; mechanical properties: $E=10796kg/mm^2$, $\sigma_b=107kg/mm^2$, $\sigma_y=93.6kg/mm^2$, $\delta=9.4\%$, $K_c=372.4kg/mm^{3/2}$ [16], $\Delta K_{th}=205.4kg/mm^{3/2}$ [17].

The test sample is a 300x100x2mm central penetration tensile type. The section which the crack passes through carries out local polishing.

The fatigue tests are carried out on a Schenk PC-160M electrohydraulic servo-fatigue tester. The overload process was controlled by an SPC-16/40 computer. The test parameters were: constant load ratio R-160kg/1600kg=0.1, frequency f=10Hz; single tensile overload, overload ratio $r=P_{oL}/P_{cA}$=1.3, 1.4, 1.5, 2.0, 2.4, 2.66, 2.8, f=0.03Hz, overload crack length 2a=32mm, etc.

We observed the crack tip and fracture by taking pictures with a photographic microscope, a micro-interferometer and a scanning electron microscope. We carried out observation of the overload crack tip film using a transmission electron microscope and 200KV and double beam conditions. The film preparation process was: the test sample with crack tips was cut along the thickness direction with an electric spark into 20x20x0.15mm slices, insulating cement was used to protect the crack tips and after chemical thinning until the thickness was about 40 micron, it is again thinned to local perforation on a double spray electrolytic polisher so that the hole circumferences were about 2000Å to enable observations.

III. Test Results

3.1 Effects of Overload Ratio on the Fatigue Crack Growth Rate

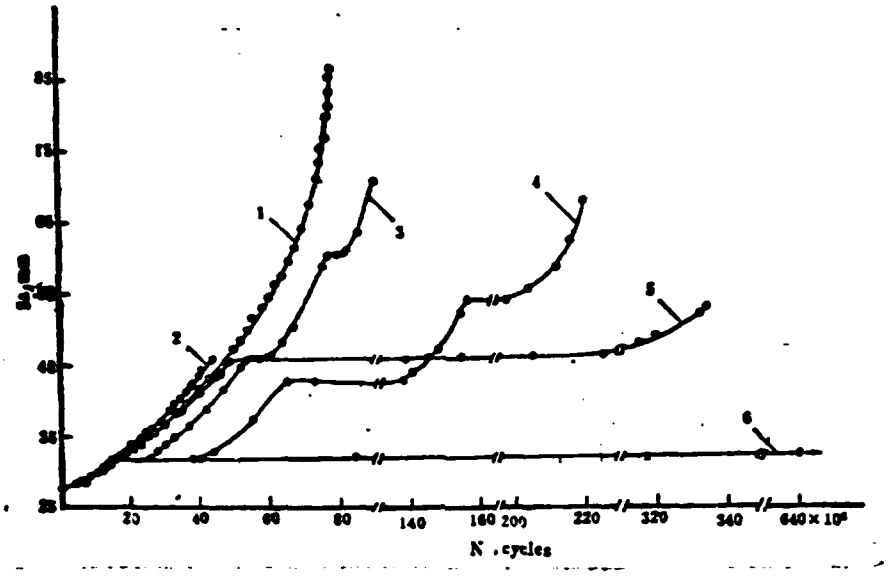

Fig. 1 Effects of overload ratio on the fatigue crack growth rate.

Key: 1. r=1.0; 2. r=1.4; 3. r=2.0; 4. r-2.4; 5. r=2.66; 6. r=2.8.

It can be seen from Fig. 1 that the effects of different overload ratios on fatigue crack growth rate are noticeably different. In carrying out overloading in a 2a=32mm area, when r=1.4, we are almost unable to see any effect; when r=2.0, noticeable retardation effects are produced. Because the retarded and increased cycle number N_D is about 15,000 times, when r=2.4, N_D is about 30,000 times; when r=2.66 (2a=46mm), N_D reaches about 150,000 times, and when r=2.8, crack growth is extremely slow and is close to a halted state.

3.2 Changes of Crack Tip Zone After Overloads of Different Ratios

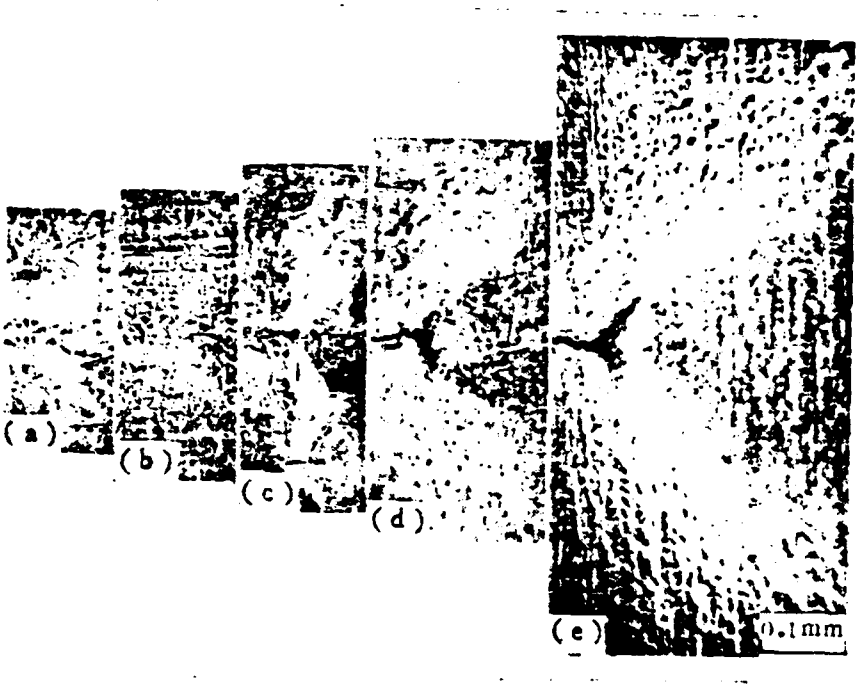

Fig. 2 (Plate 12) Passivation and deformation of crack tip after overloads of different ratios.

Key: (a) r=1.0; (b) r=1.5; (c) r=2.0; (d) r=2.4; (e) r=2.8.

It can be seen from Fig. 2 (see Plate 12) that noticeable differences exist in the passivation of crack tips after overloads of different ratios. Under constant loads, crack tips are very sharp and after overloading 1.5 times, the changes are relatively small. However, after overloading 2.0 times, the crack tips have noticeable opening and passivation. After overloading 2.4 times and 2.8 times, the level of tip opening and passivation successively and noticeably increases.

After overloading with different ratios, the plastic deformation near the crack tip is as shown in Figs. 2 and 3 (see Plate 12). It can be seen from the figures that the plastic deformation zone and level near the constant load crack tips are very small.

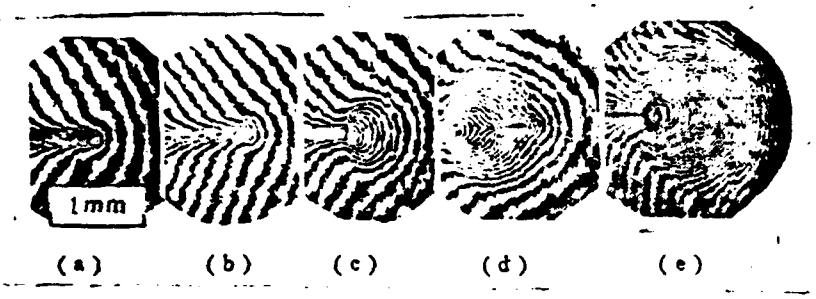

Fig. 3 (Plate 12) Changes of the plastic zone near the crack tip after overloads of different ratios.

Key: (a) r=1.0; (b) r=1.5; (c) r=2.0; (d) r= 2.4; (e) r=2.8.

The changes after overloading 1.5 times are also not large yet "wing shaped" concentrated deformation zones extending towards the two front sides have already begun to appear. After overloading 2.0 times, the "wing shaped" deformation zone clearly enlarges, the dimensions of the plastic zone correspondingly increase and the shape gradually becomes round. After overloading 2.4 times and 2.8 times, the above changes are even more evident (among them, after overloading 2.4 times, growth continues for a distance under constant load and therefore has effects on the deformation conditions within the overload plastic zone). From the changes of the density of the interference fringes in Fig. 3, we can see that following the rise of the overload ratio there are gradual and noticeable increases in the deformation level and gradient of the two front sides of the crack tip. However, the deformation gradient of the tip area just in front gradually decreases. This corresponds completely with the deformation conditions near the tip as shown in Fig. 2. See Fig. 4 for the distribution of the plastic strain of the sample's thickness direction in the plastic zone just in front of the crack tip zone after overloads of different ratios. The figure quantitatively shows the conditions of the above mentioned changes.

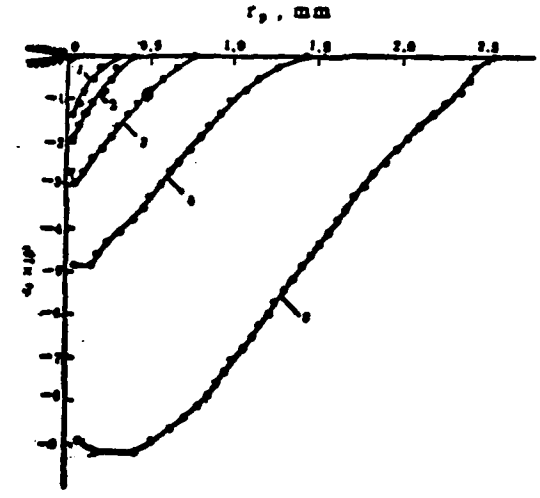

Fig. 4 Distribution of the plastic strain (ε_3) in front of the crack tip after overloads of different ratios.

Key: (1) r=1.0; (2) r=1.5; (3) r=2.0; (4) r=2.4; (5) r=2.8.

3.3 Changes of the Dislocation Configuration in the Plastic Zone in Front of the Crack Tip After Overloads of Different Ratios

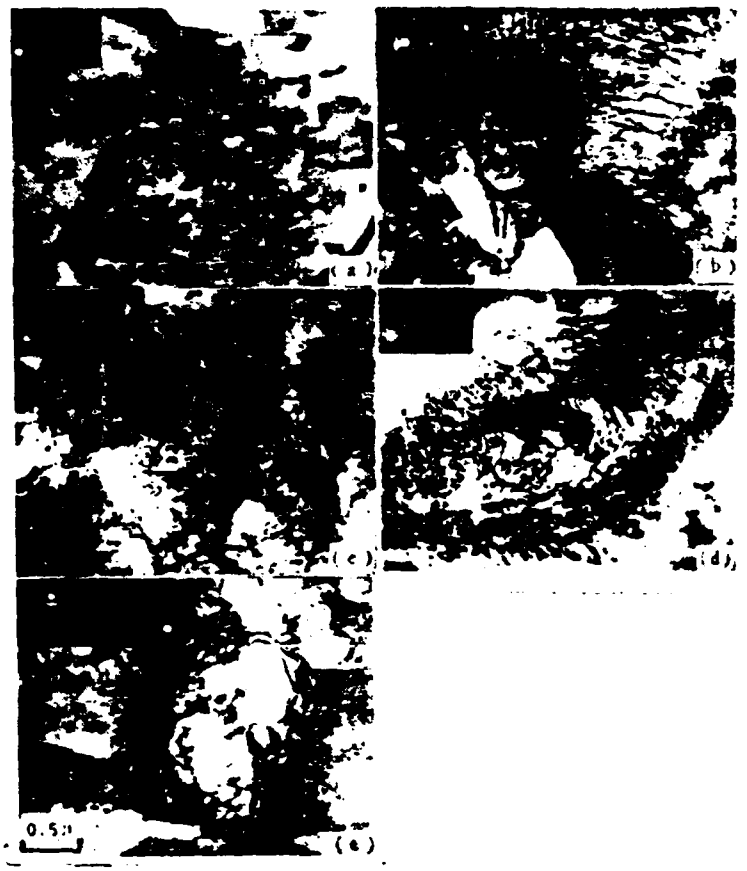

Fig. 5 (Plate 13) Plastic zone dislocation configuration within 0.3mm from the crack tip.

Key: (1) Original state.

It can be seen from Fig. 5 (see Plate 13) that there are only a small number of dislocation lines arranged in a scattered manner in the originally annealed sheets. However, the number and density of dislocation lines noticeably increases in the crack tip plastic zone with constant load fatigue (the same as the tip distance less than 0.3mm) and the local area has a dislocation network. This indicates that the cyclic hardening process has already occurred which causes the dislocation to have relatively noticeable increase. After overloading 1.5 times,

many block (round) shaped dislocation network structures appear and their densities are correspondingly raised. After overloading 2.0 times, the plastic strain near the tip enlarges and the process of cyclic hardening increases and begins to form cellular dislocation structures. However, at this time, the dimensions of the cells are not very large, the cell walls are relatively thin and many irregularly arranged dislocation lines still exist inside the cell. Yet, after overloading 2.8 times, the cyclic strain and hardening level both noticeably enlarge near the tip and thus the dislocation cell structure is even more complete and distinct. Moreover, the dimensions of the cell decrease, the thickness of the wall increase, the dislocation density increases and the dislocation in the cell noticeably decreases.

3.4 Observations of Crack Closure Phenomena in the Overload Plastic Zone

Fig. 6 Crack closure effects in the overload (r=2.4) plastic zone. (see next page for Key)

Fig. 6 Key: (a) Appearance of crack before and after overloading; (b) Appearance of plastic zone corresponding to (a).

It can be seen from Fig. 6 (see Plate 13) that after overloading 2.4 times, relatively large plastic deformation and plastic zone appear in front of the crack tip. When the crack continues to grow under constant load, the section of crack near the overload crack tip still maintains a closure state. At the same time, it can be seen that no noticeable plastic deformation traces are produced on the two sides of the crack. After the crack grows a certain distance, its tip gradually produces, increases and restores plastic deformation under constant load and the crack closure level also correspondingly and gradually lowers.

3.5 Changes in the Appearance of Fractures Before and After Overloads of Different Ratios

The fracture surface records the changing process before and after overloads of different ratios near the leading edge of the entire crack inside the test sample. We can see from the macroscopic views of the fractures shown in Fig. 7 (see Plate 14) that the fractures growing under constant loads are basically all plane strain types and there are no shear inclined planes. When there is overloading, the two sides of the test sample have, to different degrees, inclined fracture sections. Following the rise of the overload ratio or the increase of the overload crack length, the growth of the section increases under overload cycles. Because of the growth and decline of the plane strain and plane stress sections, the overload growth line gradually changes into a triangle from the forward protruding circular arc. After overloading, the crack growth then begins to take precedence from the surface layer. Later, it is then the internal and intermediate sections until the leading edge of the crack is gradually restored to the radian under constant load and forms a "saddle shaped" retardation growth zone. The

surface of the fracture is relatively level and smooth. By measuring the length of the changed appearance of the fracture, we can obtain decelerated retardation and the crack length of the entire retarded growth. After overloading 2.4 times, the measured decelerated growth distance was about 0.25mm which is about 1/5 of the diameter of the overload plastic zone.

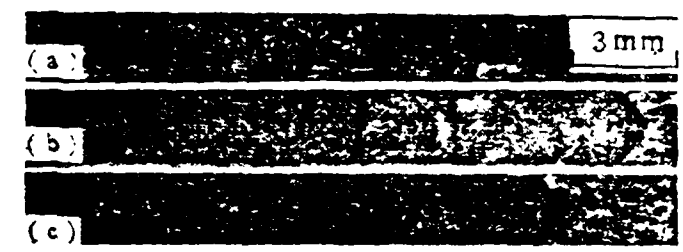

Fig. 7 (Plate 14) Macroscopic views of fractures.
Key: (a) r=1.0; (b) r=2.0; (c) r=2.4.

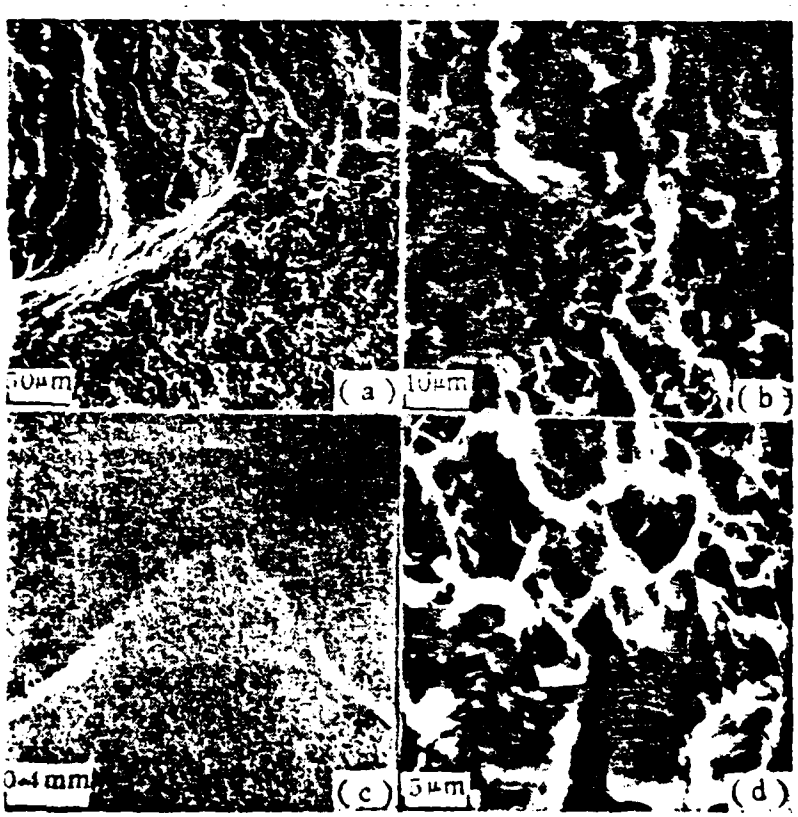

Fig. 8 (see next page)

Fig. 8 Macroscopic views of fractures before and after overloading (2a=60mm, r=2.0).

Key: (a) Before and after surface layer overloading; (b) When there is internal overloading and after overloading; (c) Entire appearance of fracture before and after overloading; (d) Before internal overloading and during overloading.

The macroscopic views of the fractures before and after overloading (Fig. 8, see Plate 14) show that the surface layer cracks before and after overloading are basically the fringe growth mechanism under plane strain conditions. When there is overloading, concentrated shearing deformation occurs under plain stress conditions yet it generally does not initiate crack growth. When there are internal cracks before and after overloading and during overloading, then there is growth throughout under plane strain conditions. Prior to overloading there is the typical fringe mechanism, during overloading there is the tough nest mechanism and after overloading there is the fringeless or precise fringe mechanism similar to the early period of fatigue.

IV. Discussion

We can see from the above test results that following the rise of the overload ratio, the overload crack tip gradually changes from sharp to coarse and dull and the tensile plastic strain quantity surrounding the tip and the dimensions of the plastic zone gradually increase; on the other hand, the dislocation configuration in the overload plastic zone also noticeably changes with the rise of the overload ratio and the dislocation density also correspondingly rises. At the same time, we can also see from the appearance of the fractures before and after the overload that following the rise of the overload ratio, the cracking and deformation of the overload crack tip also enlarge. Following this, the crack length of the retarded growth and the resulting increased cycle number also correspondingly increase. Figure 9 shows the relationship

between the maximum strain of the crack tip after overloading, plastic zone diameter and increased cycle number due to delay effects and the overload ratio. It can be seen from the figure that their numerical values, which increase with the overload ratio, form an index relation rise. At the beginning, the overload ratio of the measured retardation effects is about 1.5 but the critical value which causes the cracking to basically stop is about 2.8. This law of change is basically identical to the results we obtained in LY12 sheet aluminum alloy.

It is very clear that the delay effects are more noticeable following the rise of the overload ratio. The source of this lies in the differences in the plastic deformation range and level caused by the different overload ratios near the crack tip. However, the larger the plastic strain quantity, the larger the residual compression stress produced for the plastic zone when the elastic deformation of its surrounding expanded area of materials is restored; moreover, the larger the dimensions of the plastic zone, the larger the range of the stress. It is just this residual compression stress which has a double effect on later crack growth: it compresses the material and blocks crack extension in front of the crack tip; but after cracking, it then presses down the material behind the crack and blocks the cracks from opening up.

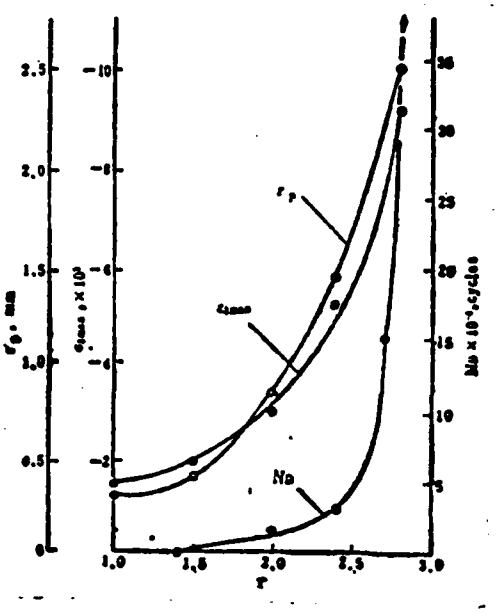

Fig. 9 Relationship between the overload's plastic zone diameter (r_p), the maximum strain of the crack tip (ε_{3max}), the increased cycle number (N_D), and the overload ratio (r).

This work shows that when the overload ratio is sufficiently large, the residual compression stress near the overload crack tip is quite large. There is not only a noticeable delay in its growth rate during cracking but also after cracking this section of cracking is in different levels of closure state for a long time. In order to differentiate the different relative positions, different processes and different effects of the residual compression stress, we separately called them residual compression stress and closure (opening) stress and primarily proved that the effects of these two residual stresses greatly lowered the effective stress strength factor amplitude of the crack tips which caused a noticeable retardation of the crack growth rate. However, because of the closure stress of the crack tip after entering the overload plastic zone, after instantaneous lowering, there existed a process of first increasing progressively and then decreasing progressively which

caused the crack growth rate to have corresponding deceleration retardation and a gradual restoration process [2].

This work further showed that following the rise of the overload ratio, the transformation process of the dislocation configuration and density of the overload crack tip is basically the same as the fatigue hardening process caused by the metallic material with relatively high fault energy (relatively easy cross slip) which follows the stress amplitude rises and cycle number increases [18]. That is, following the rise of the overload ratio, the hardening level caused by the overload cycles gradually rises until after overload 2.8 times wherein clear cellular structures are produced. This shows that it has already basically reached the saturated cycle hardening level of this material under relatively high stress range. We can see from this that the material hardening caused by overload plastic zone dislocation configuration changes and density rises also make a certain contribution to overload retardation effects. Because when there is dislocation movement there is interaction between the solute atoms, point defects and especially the dislocation stress field, the advancing resistance increases. The higher the dislocation density, the larger the resistance. In order to cause the materials to continue to deform and cause the cracks to continue to grow, it is necessary to raise the additional stress so as to cause it to be greater than the entire internal stress, that is, $\sigma > \sum \sigma_i$. This causes the dislocation in the movements to be able to overcome the various stress fields with different ranges [19].

Therefore, the relatively large plastic strain and strain zone produced by the overload cycles not only raised the residual compression stress in front of the crack tip and closure stress behind the crack tip and lowered the effective stress strength factor, but, at the same time, the configuration changes and density increases of the dislocation caused overload plastic zone hardening and raised the resisting power

against the material continuing to deform and the cracks continuing to grow. This then results in three major factors of overload retardation effect. Figure 10 is a schematic diagram of the process and mechanism of tensile overload retardation of crack growth.

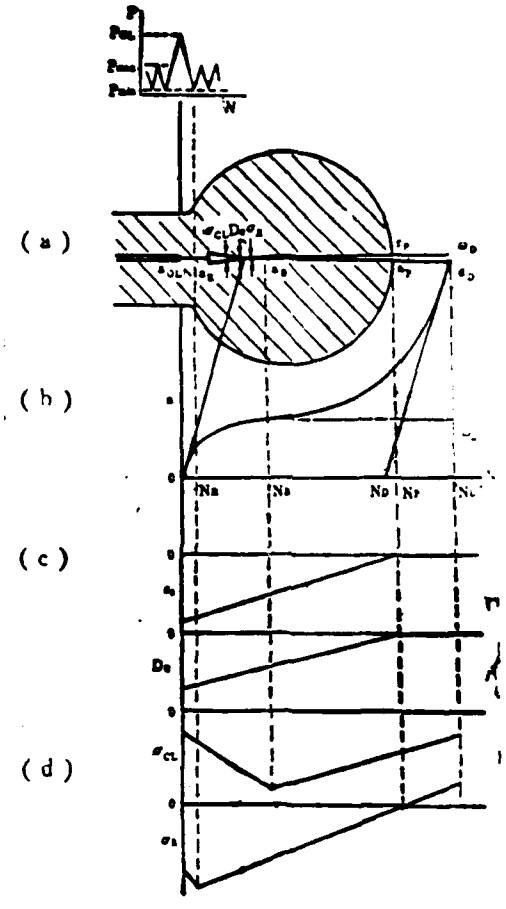

Fig. 10 Schematic diagram of process and mechanism of tensile overload retardation of crack growth.

Key: (a) Process of crack retardation growth after overload; (b) Crack growth rate (a-N) curve after overload; (c) Strain distribution after overload; (d) Major factors and other acting processes producing retardation effects.

The figure shows: (a) the changes of the plastic zone after overloading and the process of crack retardation effect:

$a_{OL}-a_B$, a_B-a_D, $a_{OL}-a_p$ and $a_{OL}-a_D$ are separately the deceleration stage, recovery stage, overload plastic zone and entire retardation zone growth; (b) the crack growth rate curve after overloading: N_B, N_R, N_D* and N_D are separately the deceleration stage, plastic zone, retardation zone and the number of cycles increased because of retardation; (c) the distribution of the overload plastic strain (ε_3); (d) the major factors producing retardation effects and their action processes, σ_R, σ_{cL} and D_e are separately the residual compression stress, closure stress and dislocation density. Among these, the closure stress acts for a long time in the entire retardation zone and it is the most important factor (after tightly connected overloading, except for the small number of cycles spontaneously lowered due to crack tip passivation effects); the residual compression stress and overload cycle hardening in front of the crack tip are then only in the overload plastic zone and mainly act in the deceleration stage. There are other factors besides these such as crack tip passivation; when there is overloading, the concentrated shearing strain under plane stress conditions is in contradiction to the low stress strength after overloading and requires growth under plane strain conditions which causes an approximately 45° turn of the crack growth direction; the section of growth under overload is rough and uneven (beneficial in raising the closure stress) etc. All of these factors possibly contribute, to different degrees, to the retardation effect.

We can also see from Fig. 9 that the maximum strain in front of the crack tip, ε_{3max} and the overload plastic zone diameter, and r_p are completely identical in their tendency to change with the overload ratio, that is, $\varepsilon_{3max} \propto r_p$. Thus, we can obtain the following relational formula:

$$\varepsilon_{3max}=k\cdot r_p \qquad (1)$$

In the formula, k is the geometrically related constant of the

material and test sample, $k=(-4)\times10^{-3}mm^{-1}$; $r_p=\frac{1}{d\pi}\left(\frac{\Delta K_{OL}}{\sigma_{ya}}\right)^2$.

In this expression, ΔK_{OL} is the overload's stress strength factor range, d is the stress condition parameter, $1 < d < 3$.

At the same time, we can see from Fig. 9 that the cycle number N_D which increased because of the retardation effects changes with overload ratio r and becomes the index relation. Actually, the source of this is in the changes of the ratio of the overload plastic zone and dimensions of the constant load plastic zone,

$$\frac{1}{d\pi}\left(\frac{\Delta K_{OL}}{\sigma_{y.s}}\right)^2 \Big/ \frac{1}{d'\pi}\left(\frac{\Delta K}{\sigma_{y.s}}\right)^2 = \frac{d'}{d}\left(\frac{\Delta K_{OL}}{\Delta K}\right)^2 = m'r^2$$

Therefore, we can obtain a simple empirical expression:

$$N_D=N_O\exp(mr^2) \qquad (2)$$

In the formula, N_O and m are the geometrically related test constants of the material and test sample, and r is the overload ratio. From formula (2) we obtain

$$\ln N_O=\ln N_D+mr^2$$

We can see from Fig. 11 that N_D and r^2 separately form a linear relation between the three zones showing that N_D has different growth rates within each zone of r=1.0～2.0, r=2.0～2.7 and r=2.7～3.0. At the same time, it shows that when the overload ratio is greater than 1.5, the retardation effect is very small yet there does not exist the overload threshold value at the beginning of the production of the retardation effect. When the overload ratio approaches 3.0, the cracks will stop.

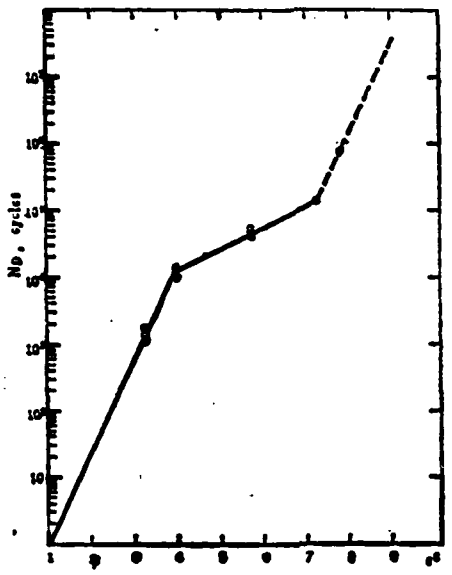

Fig. 11 Relationship of overload increased cycle number N_D and overload ratio r^2.

V. Conclusions

1. Overloads with different ratios have different effects on the fatigue crack growth rate. When the overload ratio is larger than 1.0 but smaller than 1.5, the retardation effect is very small and is generally difficult to measure. When the overload ratio approaches 3.0, this will cause the cracks to stop growth.

2. The major factors of tensile overload producing retardation effects are the relatively large residual compression stress, closure stress and cycle hardening caused by the overload plastic zone. Closures stress and residual compression stress separately prevent crack opening in back of the crack tip and block crack extension in front of the tip; cycle hardening raises the resisting power of the material against continuing deformation as well as the stress strength level

required for the crack to continue growth.

3. We obtained empirical expressions for calculating the maximum plastic strain (ε_{3max}) of the overload crack tip and the cycle number (N_D) increased because of the overload retardation effect.

References

[1] Hudson, C.M. and Raju, K.N., NASA TN-D-5702, 1970.

[2] Ouyang Jie and Yan Minggao, Proc. 1st China-USA Bilaternal Metal. Conf., Beijing, 1981, 418 or Journal of Metallurgy, 13(1982), No. 1, P. 38.

[3] Von Euw, E.F.J., Hertzberg, R.W. and Roberts, R., ASTM STP 513, 1972, 230.

[4] Jones, R.E., Eng. Frac. Mech., 5(1973), 585.

[5] Nelson, Drew V., Exper. Mech., Feb. 1977, 42.

[6] Christensen,R.H., Metal Fatigue, McGraw-Hill, New York, (1959), 385.

[7] Schijve,J. and Broek, D., Aircraft Engineering, 34(1962),314.

[8] Taira,S., Tanaka, K. and Yamasaki, T., Soc. Mater. Sci., Japan, 27(1978), 251.

[9] Wheeler, O.E., Trans. ASME, ser. D.,J.Basic Eng.,94(1972),181.

[10] Elber, W., ASTM STP 486, (1971), 230.

[11] Schijve, J., Eng. Frac.Mech., 11(1979), 182.

[12] Willenborg, J., Engle,R.M. and Wood,H.A. AFFDL-TM-71-1-FBR, (1971).

[13] Matsuoka,S. and Tanaka,K., Eng.Frac.Mech. 8(1976),3,50.

[14] Matsuoka,S. and Tanaka,K., Eng.Frac.Mech.10(1976),3,515.

[15] Maarse,J., Fracture Vol.2, ICF4, (1977), 1025.

[16] Wanhill, R.J.H. and Others, Interim Report No.5,1M1 318,1974.

[17] Gray,T,D., and Gallagher,J.P., ASTM STP 590, 1976, 331.

[18] Klesnil, M. and Lukas, P., Fatigue Metallic Materials, Elsevier Scientific Publishing Company, Amsterdam-Oxford-New York, 1980, 30.

[19] Argon, A.S., Mater, Sci.Eng. 3(1968/69), 24.

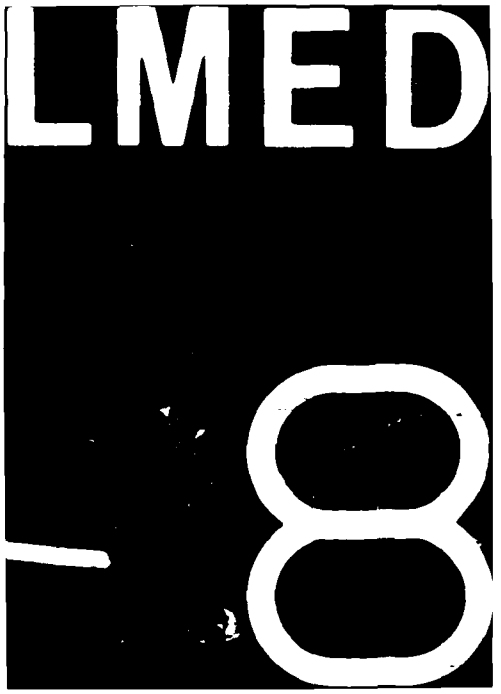
LMED
8